catalysts

MDPI

Article

Ammonium Phosphotungstate Bonded on Imidazolized Activated Carbon for Selective Catalytic Rearrangement of α-Epoxypinane to Carveol

Min Zheng [1,2], Xiangzhou Li [1,3,*], Dulin Yin [4,*], Steven R. Kirk [4], Hui Li [5], Peng Zhou [1] and Yanhong Yang [1]

1 College of Materials Science and Engineering, Central South University of Forestry and Technology, Changsha 410004, China; zhmmjf@126.com (M.Z.)
2 School of Elementary Education, Hunan First Normal University, Changsha 410205, China
3 Institute of Natural Products Processing and Utilization, Central South University of Forestry and Technology, Changsha 410004, China
4 National & Local Joint Engineering Laboratory for New Petro-Chemical Materials and Fine Utilization of Resources, Hunan Normal University, Changsha 410081, China
5 Xining Center of Natural Resources Comprehensive Survey, CGS (China Geological Survey), Xining 810008, China
* Correspondence: RLXZ@163.com (X.L.); dulinyin@126.com (D.Y.)

Abstract: Carveol is a rare fine chemical with specific biological activities and functions in nature. The artificial synthesis of carveol from plentiful and cheap turpentine is expected to further improve development of pharmaceutical and industrial applications. A new green catalytic system for the preparation of high-value carveol from α-epoxypinane is presented. A novel ammonium salt solid acid (AC-COIMI-NH_4PW) was obtained from phosphotungstic acid bonded with imidazole basic site on nitrogen-doped activated carbon which, after ammonia fumigation, presented an excellent catalytic performance for the selective rearrangement of α-epoxypinane to carveol in DMF as solvent under mild reaction conditions. At 90 °C for 2 h, the conversion of α-epoxypinane could reach 98.9% and the selectivity of carveol was 50.6%. The acidic catalytic sites exhibited superior durability and the catalytic performance can be restored by supplementing the lost catalyst. Based on the investigation of catalytic processes, a parallel catalytic mechanism for the main product was proposed from the rearrangement of α-epoxypinane on AC-COIMI-NH_4PW.

Keywords: catalytic rearrangement; α-epoxypinane; carveol; ammonium phosphotungstate; activated carbon

Citation: Zheng, M.; Li, X.; Yin, D.; Kirk, S.R.; Li, H.; Zhou, P.; Yang, Y. Ammonium Phosphotungstate Bonded on Imidazolized Activated Carbon for Selective Catalytic Rearrangement of α-Epoxypinane to Carveol. *Catalysts* **2024**, *14*, 36. https://doi.org/10.3390/catal14010036

Academic Editor: Piotr Kuśtrowski

Received: 6 December 2023
Revised: 30 December 2023
Accepted: 31 December 2023
Published: 3 January 2024

1. Introduction

Carveol, as a fine chemical of monocyclic monoterpenes, is widely used in food and daily flavoring additives [1], as well as in the research of constructing a chemical improvement on mercury-induced oxidative stress and neurodegeneration animal model [2]. It is also a raw material for the synthesis of dihydrocarveol which has more applications [3]. In nature, carveol only presents in very small amounts in the essential oils of herbaceous plants such as Artemisia annua and spearmint. The early production of carveol was achieved by hydrogenation of carvone extracted from plants such as spearmint. The content of carvone in the leaves of spearmint is only 0.1–0.5% [4,5], and the content in the roots of spearmint is much lower [5], which indicates that the natural source of carveol is rare.

Turpentine oil, which can be separated from pine resin deposited through photosynthesis in pine leaves, represents the largest production of terpene essential oil worldwide and is a widely used synthetic intermediate [6,7]. In recent years, academia and industry have attached greater importance to the preparation of a large number of monoterpene-based bio-derivative functional products from turpentine oil [8,9]. Among them, α-pinene, the main component in turpentine, can be oxidized and derived into α-epoxypinane [10–12], which

is a highly reactive tricyclic monoterpene oxygenate with a ternary oxygen-containing heterocycle and a quaternary carbon ring. In the presence of acid catalysts, α-epoxypinane (APO) is usually rearranged into campholenic aldehyde (CA) and fencholenic aldehyde (FA) with a five-membered ring (C5), or carveol (CV), menthadienol (MD) with a six membered ring (C6) in two pathways (Scheme 1) [13,14]. Selective catalytic rearrangement of α-epoxypinane has, therefore, become an exciting challenge in the research towards using this process to manufacture fine chemicals [15,16]. Focusing on the development of the green chemical industry, most scientists have carried out solid acid catalytic α-epoxidepinane rearrangement, such as a copper salt supported on metal organic framework MOF-25 [17], a bi-functional PrAlPO-5 molecular sieve [18], an acidified clay [19], a mesoporous molecular sieve supported iron catalyst [20], a modified natural zeolite [21], phosphate functionalized carbon spheres [22], MoO_3-modified zeolite BETA [23], etc. In these works, much attention has been paid to direct the reaction towards the production of C5 (CA). There is rarely work on the selective synthesis of CV (C6 product) from the catalytic rearrangement of α-epoxypinane.

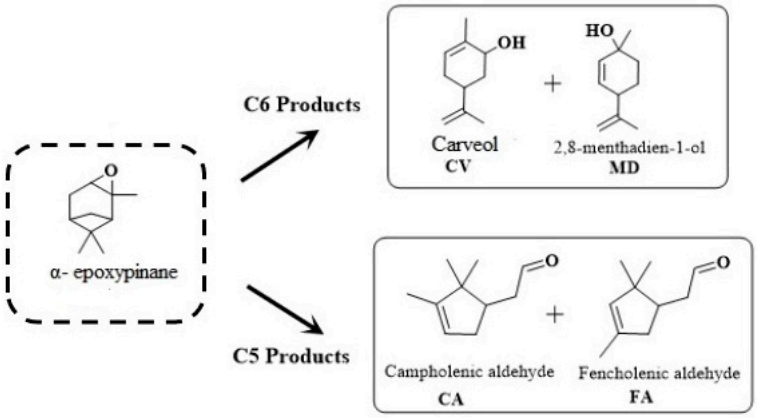

Scheme 1. Main pathway of α-epoxypinane rearrangement.

In our previous work, it was found that imidazolated nitrogenated activated carbon anchoring phosphotungstate had excellent catalytic performance for benzyl alcohol [24], and the reaction of α-pinene with hydrogen peroxide on ammonium phosphotungstate immobilized on imidazolated nitrogenated activated carbon could selectively convert to sobrerol [25]. In present work, ammonium phosphotungstate anchored by imidazolated nitrogenous activated carbon was developed to catalyze α-epoxypinane ring-opening rearrangement, so as to improve the selective synthesis of carveol and provide a new green [26] catalytic material system from biomass based activated carbon for the preparation of high-value carveol from plentiful and cheap turpentine.

2. Results and Discussion

2.1. Structure and Texture Characteristics of Catalysts

The FTIR spectrum and XRD of activated carbon (AC), phosphotungstic acid supported on imidazolized AC (AC-COIMI-HPW), and ammonium phosphotungstate anchored by imidazolized AC (AC-COIMI-NH_4PW) is shown in Figure 1A. The FTIR spectrum of AC in Figure 1A showed that the absorption peaks at 1608 cm^{-1} and 1400 cm^{-1} attributed to C=C stretching vibration of the cyclic aromatic skeleton in AC, and there is the characteristic absorption peak of -OH linked at the edge of fused polycyclic aromatic in the bulk of AC at 3130 cm^{-1}. Compared to AC, the FTIR spectrum of AC-COIMI-HPW showed characteristic peaks of N-H, C-N, P-O, W-O-W, W-O, and P-W at 1710 cm^{-1}, 1202 cm^{-1}, 1077 cm^{-1}, 981 cm^{-1}, 893 cm^{-1}, and 812 cm^{-1}, respectively. The characteristic peak at 522 cm^{-1} was the characteristic absorption of acyl imidazole, similar to a tertiary amide [27]. A broad absorption of N-H of imidazole ammonium salt appeared between 3360 cm^{-1} and 3000 cm^{-1}. Furthermore, the absorption peak at 1600 cm^{-1} was significantly enhanced,

which was attributed to the increased C=O stretching vibration peak after oxidation overlapping with the peak of the carbon skeleton, and the peak appeared to be blue shifted, indicating that HPW successfully introduced the imidazolated activated carbon surface alkaline site. The AC-COIMI-HPW was ammoniated into AC-COIMI-NH_4PW, and the symmetric and asymmetric stretching vibration absorption of NH_4^+ between 3360 cm^{-1} and 3000 cm^{-1} was enhanced. No significant Keggin structure HPW absorption peak was found in the catalyst, confirming that the phosphotungstate was highly dispersed, which is also consistent with the XRD results.

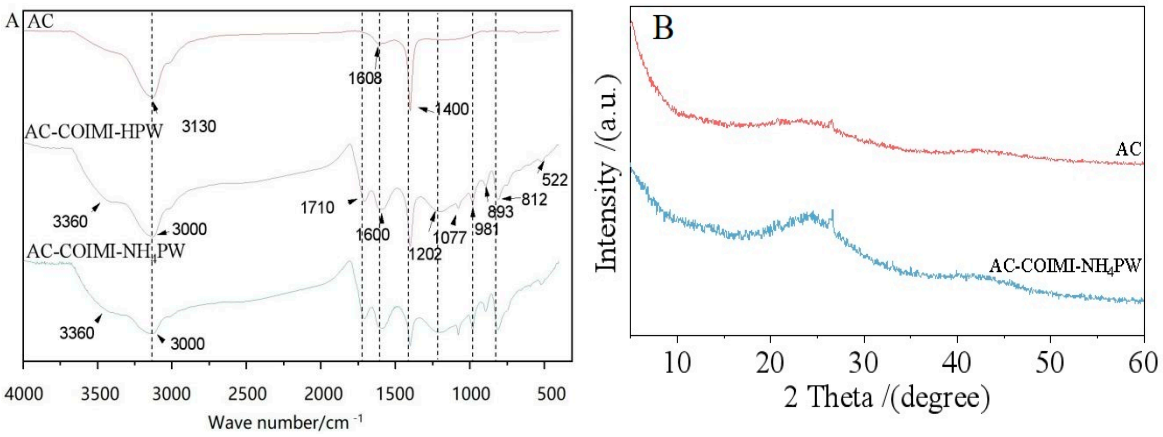

Figure 1. The FTIR (**A**) and XRD (**B**) spectrum of AC, AC-COIMI-HPW, and AC-COIMI-NH_4PW.

The XRD result in Figure 1B only displayed both the amorphous phase diffraction characteristics of AC and AC-COIMI-NH_4PW, and no obvious diffraction peaks corresponding to ammonium phosphotungstate are observed due to its low content in the catalyst. This observation indicates that the ammonium phosphotungstate is highly dispersed on the surface of the activated carbon through single-molecule chemical adsorption on the basic imidazole sites [28].

Figure 2 showed the full XPS spectrum and the deconvolution of C 1s, N 1s and W 4f in AC, AC-COIMI-HPW, and AC-COIMI-NH_4PW. Compared to AC, it is indicated that XPS absorption of C1s at 288.5 eV belongs to C=N bonds in AC-COIMI-HPW, and AC-COIMI-NH_4PW, which originated from the imidazolization of the oxidized activated carbon. It also can be seen that obvious XPS absorption of W $4f_{5/2}$ and W $4f_{7/2}$, respectively at 38.3 eV and 36.2 eV consistent with XPS absorption after adsorption of ammonium phosphotungstate on heterocyclic nitrogen of carbon nitride C_3N_4 [29], was observed after immobilization of HPW on imidazolized activated carbon AC-COIMI and subsequent ammoniation to -NH_4PW species in AC-COIMI-HPW. In the phosphotungstate anion, the phosphorus atom is in the central position, while tungsten atoms are connected by oxygen bridges. The conversion of acidic H^+ to NH_4^+ is difficult to cause a significant effect on the core electronic structure of tungsten, so the XPS of W $4f_{5/2}$ and W $4f_{7/2}$ are almost the same. Since H^+ on AC-COIMI-HPW formed NH_4^+ with NH_3, the N1s XPS from C-N=C in the weaker acidic AC-COIMI-NH_4PW is shifted to 400.2 eV from 401.0 eV in stronger acidic AC-COIMI-HPW. It is very interesting that N1s XPS from N-H in AC-COIMI-NH_4PW were 401.5 eV, which is slightly lower than 401.8 eV in AC-COIMI-HPW, but the absorption intensity is higher, originating from the binding of NH_3 with H^+ increasing the nitrogen content in the catalyst AC-COIMI-NH_4PW.

The TG result and the N_2 adsorption isotherm of AC and AC-COIMI-NH_4PW are shown in Figure 3. TG curve of two samples under ambient air atmosphere from room temperature to 200 °C was measured (Figure 3A). The rapid weight loss is observed in the first stage of the curves at 80 °C corresponds to the desorption of physically adsorbed water from both catalytic materials.

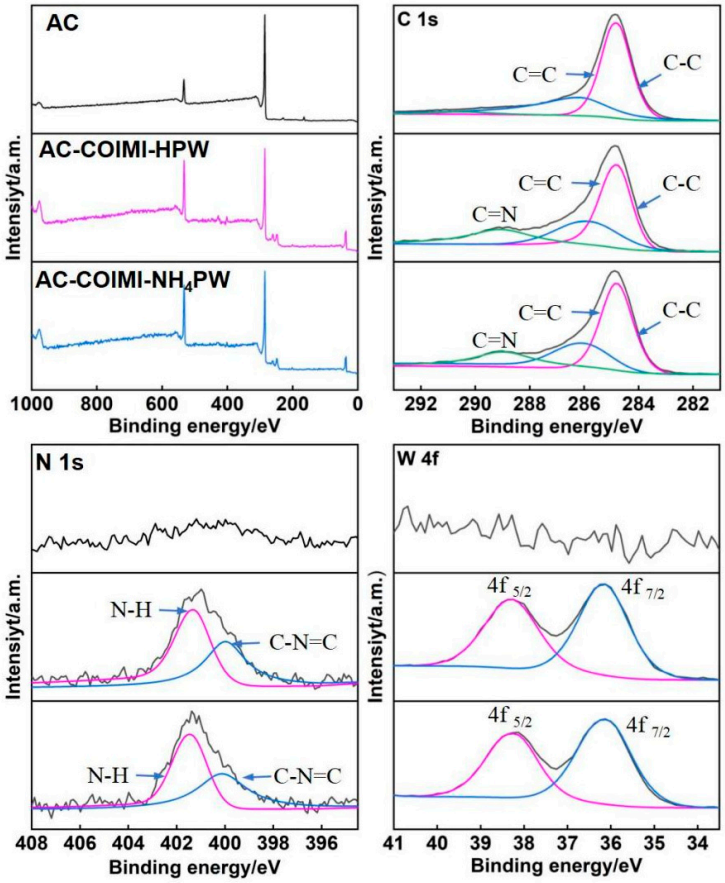

Figure 2. XPS diagram of AC, AC-COIMI-HPW, and AC-COIMI-NH_4PW.

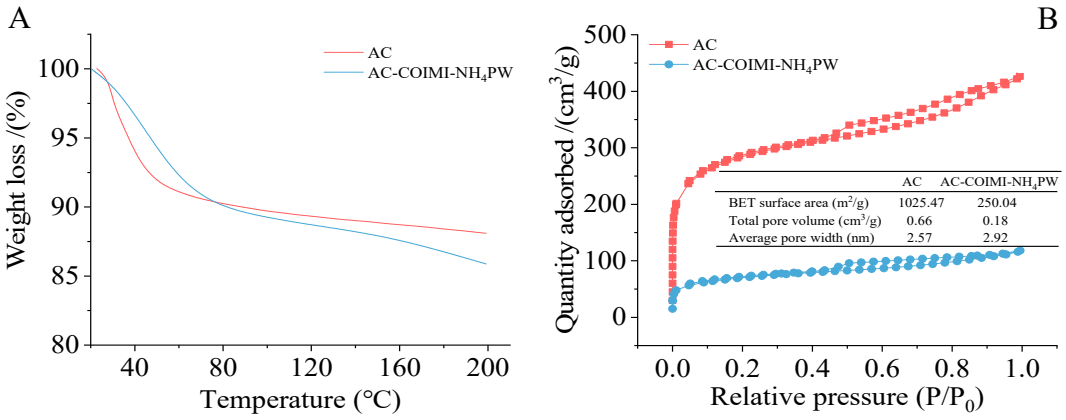

Figure 3. The TG (**A**) and BET (**B**) of the pattern of AC and AC-COIMI-NH_4PW.

The weight loss of AC-COIMI-NH_4PW is slightly higher than that of AC from TG, which may be attributed to the different amounts of water adsorption of ammonium phosphotungstate. The thermal degradation curve tends to be balanced between 80 °C and 200 °C, indicating that the catalyst has better thermal stability below 200 °C.

The textural properties of AC and AC-COIMI-NH_4PW were determined by low-temperature adsorption of N_2 (Figure 3B). The adsorption isotherms of both AC and AC-COIMI-NH_4PW exhibit type IV behavior, indicating the presence of mesoporous structures in the catalyst. After a series of chemical modifications and modifications, the texture of the activated carbon material has changed to some extent [30], with a decrease in specific surface area and pore volume, consistent with the pore structure shown in SEM.

The morphologies and microstructures of AC and AC-COIMI-NH_4PW were characterized by SEM and shown in Figure 4. It can be seen that both AC (A, B) and AC-COIMI-NH_4PW (C, D) exhibit the same texture characteristics as amorphous carbon of amorphous carbon. After oxidation treatment and imidazolated modification of AC, most of the nanofragments or particles adhering to the surface disappeared, and the surface structure of AC-COIMI-NH_4PW appeared more compact in SEM images, which contributed to maintaining the particle stability of the catalyst in the operating environment. SEM imaging further confirmed that the specific surface area of AC-COIMI-NH_4PW decreased, which was consistent with the results of BET determination.

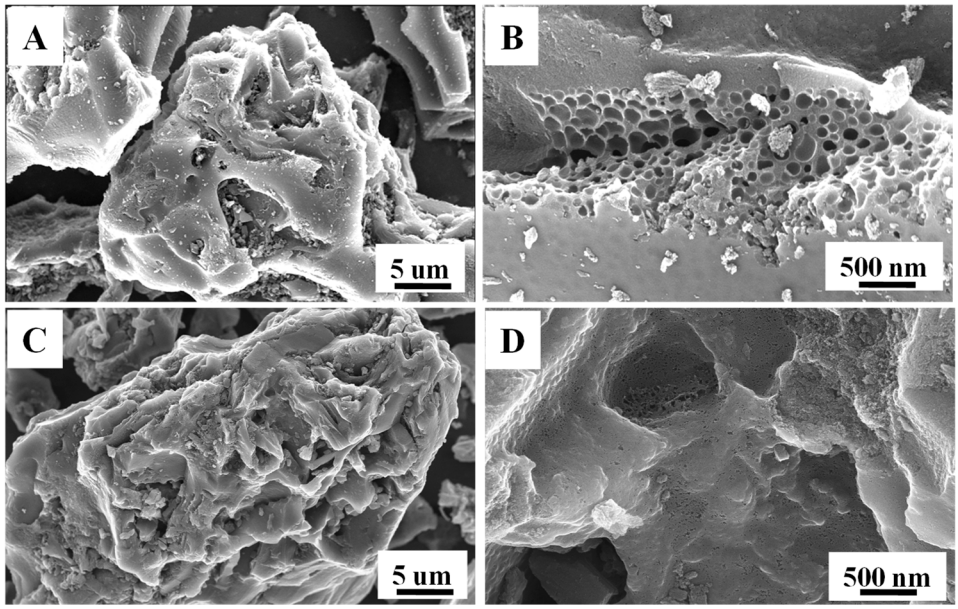

Figure 4. The SEM of AC (**A**,**B**) and AC-COIMI-NH_4PW (**C**,**D**).

2.2. Catalytic Conversion of α-Epoxypinane Rearrangement to Carveol

2.2.1. Effect of Catalysts

The catalytic performance of five different acidic catalytic materials on the liquid-phase rearrangement of α-epoxypinane to carveol under the same reaction conditions is shown in Table 1.

Table 1. Effect of different catalysts on the rearrangement of α-epoxypinane.

Catalyst	Conv. (%)	Sel. (%)				
		CA	CV	MD	FA	Others
AC	23.8	11.9	32.8	17.1	6.3	27.9
AC-COIMI-HNO_3	89.3	10.2	40.8	24.7	6.4	17.9
$(NH_4)_3PW$	98.0	12.7	44.3	28.2	5.8	9.0
AC-COIMI-NH_4PW	98.9	12.3	50.6	22.0	5.7	9.4
AC-COIMI-HPW	99.0	9.1	17.4	12.6	6.2	54.7

Reaction conditions: Catalyst 0.5 mmol, α-epoxypinane 10 mmol, DMF 10 mL, 90 °C, 2 h.

The results show that C5 products (CA and FA), C6 products (CV and MD), and some other monoterpenoid by-products could be formed over these catalysts. The -COOH proton acid site on the AC can catalyze α-epoxypinane rearrangement, but the activity is low due to the low strength of its acid center -COOH. The conversion of α-epoxypinane is only 23.8%, which is about one-quarter of that of other catalysts, the selectivity of carveol is only 32.8%, and the total selectivity of C6 products is less than 50%.

Based on the catalytic effect of imidazole nitrate on epoxypinane liquid-phase rearrangement [31], AC-COIMI-HNO_3, a supported organic imidazole nitrate salt prepared

by the adsorption of imidazolated nitro-doped activated carbon with low concentration nitric acid aqueous solution, was used to catalyze α-epoxypinane rearrangement, and showed efficient catalytic performance. The conversion of α-epoxypinane reached 89.3%, and the selectivity increased to 40.8%, but it was not as much as phosphotungstic-acid-based catalysts.

With three phosphotungstate-based catalysts, the transformation of α-epoxypinane was basically complete, but the catalytic selectivity was quite different. When the phosphotungstic acid is supported on the imidazolized AC (AC-COIMI-HPW), the effective species of the acidic active site is H_2PW^-. The proton-acid strength of H^+ in H_2PW^- is higher than NH_4^+ in $(NH_4)_2PW^-$, so AC-COIMI-HPW has stronger acid catalysis than AC-COIMI-NH_4PW. The tandem dehydration and polymerization of C6 alcohol molecules occur at the same time. The selectivity of carveol decreased from 50.6% on AC-COIMI-NH_4PW to 17.4%, and the total selectivity of C6 decreased about 40% on AC-COIMI-HPW, while the other series side reactions increased to 54.7%.

AC-COIMI-NH_4PW has the almost same catalytic activity with unloaded $(NH_4)_3$PW in equimolar quantities under the same reaction conditions, but it promotes the α-epoxypinane rearrangement towards the formation of carveol, the selectivity of carveol increased from 44.3% with $(NH_4)_3$PW to 50.6% on AC-COIMI-NH_4PW. This may be due to the presence of imidazole rings on AC-COIMI, which modulated the strength of the acid at the corresponding catalytic active site and the reaction microenvironment, thus promoting the rearrangement of α-epoxypinane to increase the selectivity of carveol on AC-COIMI-NH_4PW.

2.2.2. Solvent Modification

A liquid-solid catalytic process is more suitable for α-epoxypinane rearrangement than gas-solid catalysis at higher temperatures. The latter is more likely to dehydrate carveol to p-isopropyl toluene and to deactivate the catalyst due to covering the active site with coke through continuous oligomerization of substrates and products. The effects of different solvents on the catalytic rearrangement of α-epoxypinane on AC-COIMI-NH_4PW are shown in Table 2. It is shown that the rearrangement occurred only with difficulty when the non-polar toluene was used to composite the reaction medium with α-epoxypinane.

Table 2. Effect of solvent on α-epoxypinane rearrangement on AC-COIMI-NH_4PW.

Solvent	B.P. (°C)	Dielectric Constant	Conv. (%)	Sel. (%)				
				CA	CV	MD	FA	Others
Toluene	111	2.4	1.6	7.5	12.2	13.8	0	66.5
[a] Trichloromethane	61	4.7	5.8	8.9	9.8	17.6	0	63.7
[a] Ethyl acetate	77	6.0	3.3	7.8	12.4	16.5	0	63.3
[a] Acetone	57	20.7	7.9	21.7	11.7	6.2	0	60.4
[a] Acetonitrile	82	37.5	75.2	25.9	33.2	17.5	0	23.4
Nitromethane	101	38.6	96.1	29.8	29.5	10.7	0	30.0
DMF	153	38.7	98.9	12.3	50.6	22.0	5.7	9.4
NMP	203	48.9	95.4	20.5	43.1	17.6	4.3	14.5

Reaction conditions: Catalyst 0.5 mmol, α-epoxypinane 10 mmol, DMF, 10 mL, 90 °C, 2 h. [a]: The reaction is carried out at the boiling point of the solvent.

When ethyl acetate, chloroform, and acetone (with low dielectric constant) were used as solvents, the conversion of α-epoxypinane was still low, and the corresponding products tended to contain more unwanted by-products. The reaction rate was accelerated when the solvent was nitromethane, DMF, and NMP, which has a much higher dielectric constant, and the substrate α-epoxypinane was almost completely transformed within 2 h.

The reaction tends to produce more carveol in the latter two reaction systems, especially DMF. It might be that the special ionic bond of the catalyst active site has a large polarity on AC-COIMI-NH_4PW and is easily converted to catalytic active species in these solvents with stronger polarity, which is also similar to phosphonate functionalized car-

bon spheres as Brønsted acid [22] and other catalysts [23,32] for the rearrangement of α-epoxypinane to carveol in highly polar basic solvent. Moreover, the acidity of the catalyst can be adjusted to a great extent and more carveol can be generated when the solvent is alkaline, so DMF is more suitable for the appropriate solvent in the rearrangement of α-epoxypinane on AC-COIMI-NH_4PW.

2.2.3. Effect of Reaction Conditions

The effect of four operation conditions on the α-epoxypinane rearrangement catalyzed by AC-COIMI-NH_4PW was shown in Figure 5. Compared with the blank reaction in Figure 5A, the α-epoxypinane rearrangement rate was increased and the conversion of α-epoxypinane reached 46.7% when the amount of catalyst was 2%. The selectivity of CV and MD increased with decreasing selectivity of campholenal. When the dosage of the catalyst was increased to 5%, the α-epoxypinane was transformed completely, and the selectivity of CV also reached its highest value. When more catalyst was added, the selectivity of CV decreased slightly to other by-products.

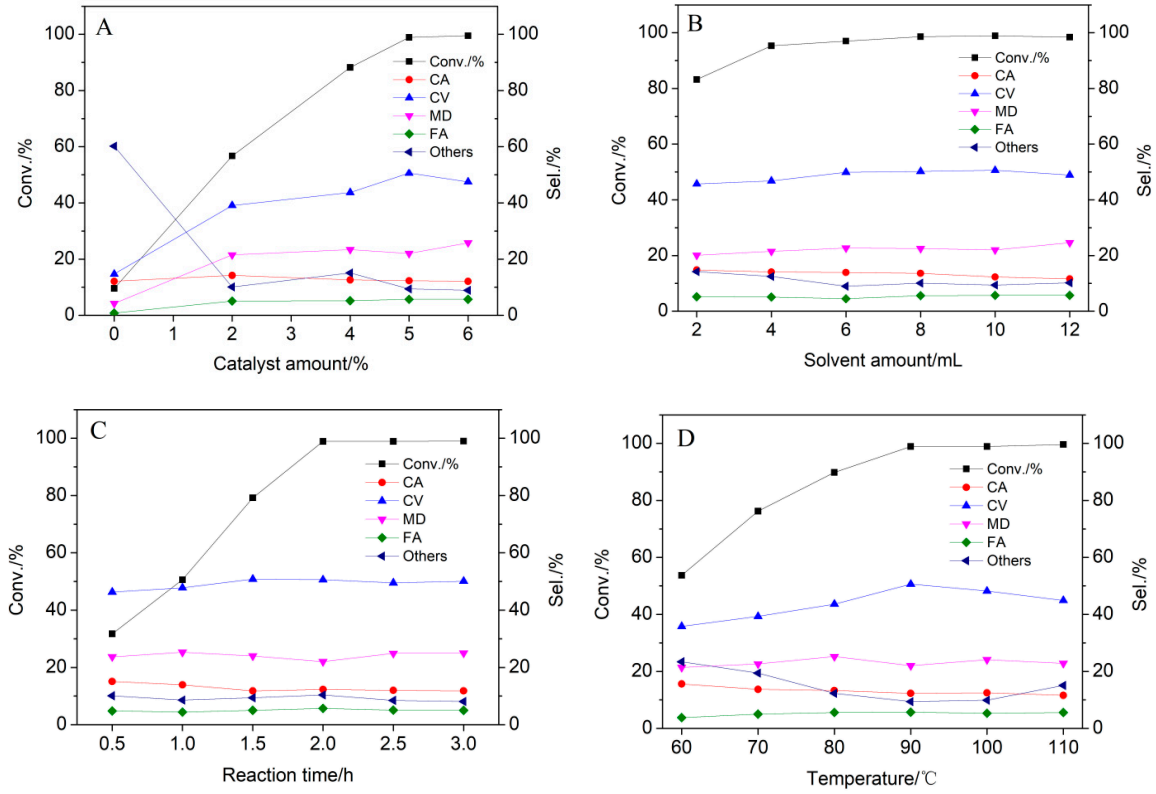

Figure 5. Effect of catalyst amount (**A**), solvent amount (**B**), reaction time (**C**) and temperature (**D**) on the rearrangement of α-epoxypinane.

The effect of the amount of solvent DMF on α-epoxypinane rearrangement is shown in Figure 5B. It can be seen that the amount of solvent in the reaction has little influence on the rearrangement. When DMF dosage increased from a total of 2 mL to a total of 6 mL, the conversion of α-epoxypinane increased from 83.2% to 98.9%, and the selectivity of CV was basically the same, indicating that the appropriate increase of solvent could improve yield to reduce the possibility of α-epoxypinane gliosis. At the same time, the increase of solvent also modifies the adsorption of the substrate on the catalytic active site, so as to form more target products (CV). With the further increase of solvent, the concentration of the substrate in the catalytic system was reduced, but the conversion of α-epoxypinane did not change significantly, from which may be deduced that the rearrangement corresponded to a quasi-zero order reaction.

From Figure 5C, it is shown that the reaction time has an initially linear effect on the α-epoxypinane rearrangement catalyzed by AC-COIMI-NH_4PW and little influence on the distribution of products. As the reaction time is increased, the concentration of α-epoxypinane in the reaction solution will inevitably continue to decrease. It is worthwhile to note that the linear increase in conversion of α-epoxypinane with reaction time means that the reaction rate is not affected by the concentration of α-epoxypinane in the liquid phase, which is characteristic of a quasi-zero order reaction. It can be inferred that the adsorption of α-epoxypinane on the solid catalyst AC-COIMI-NH_4PW remains saturated even when the concentration of α-epoxypinane decreases significantly. The reaction of α-epoxypinane adsorbed on the surface acid center of AC-COIMI-NH_4PW is a rate control step in the rearrangement process. The time increased from 0.5 h to 2 h, and the transformation of α-epoxypinane was basically complete. The selectivity of CV reached 50.6% at 2 h, and the selectivity of all products was not changed significantly by prolonging the time. It was indicated that the rearrangement exhibits the characteristic of parallel pathways in the whole reaction period. It may be that the stable carbocation from α-epoxypinane ring-opening is biased in the direction of opening the inner cyclobutene with the extension of the reaction time. The weakly alkaline and highly polar solvent DMF can promote the elimination of hydrogen atoms on the external alkyl group, causing more C6 product CV to be formed.

The effect of reaction temperature is shown in Figure 5D. The conversion of α-epoxypinane increased from 57.4% to over 98% as the reaction temperature increased from 60 °C to 90 °C and did not increase with further increasing reaction temperature due to the fact that, by this point, almost all reactants have already been converted. The selectivity of CV increased from 33.8% at 60 °C to 50.6% at 90 °C, then gradually decreased with increasing reaction temperature to 120 °C, and the selectivity of other products was increased. It is worth noting that the selectivity of the other three products did not change significantly with the increase of reaction temperature from 60 °C to 120 °C, which means that the rearrangement product was formed in a parallel reaction and was consistent with the effect of the reaction time on α-epoxypinane rearrangement on AC-COIMI-NH_4PW as shown in Figure 5C.

2.3. Catalytic Stability

The reuse stability of AC-COIMI-NH_4PW is shown in Figure 6. After being reused for 5 times, the conversion of α-epoxypinane was slightly decreased with the increase of AC-COIMI-NH_4PW cycles; however, there was little change in the selectivity of CV. It is indicated that the properties of the catalytic site was not changed because the reaction occurred under anhydrous conditions and did not involve hydrolysis of the weak acid active site NH_4^+.

Once supplemented to the initial mass, and then put into the reaction system again, the performance of the catalyst was basically restored, which reveals that the deactivation was caused by the decrease of active sites with the loss of catalyst mass.

2.4. Analysis of the Literature Data on Other Ways of Obtaining Carveol

The catalytic reactions reported in recent literature on the rearrangement of α-epoxypinane for carveol are listed in Table 3 to compare the main results of the optimal catalytic system in this work.

Table 3. Comparison of reported catalytic results of carveol from α-epoxypinane.

Substrate/Catalyst	T/°C	t/h	Conv.%	Sel. [a]/%	Times [b]	Ref.
AC-COIMI-NH_4PW	90	2	98.9	50.6	6	This work
Ce/SiO_2	140	98	98	73	1	[13]
CsPW	25	5	100	22	1	[14]
Zirconium phosphate	160	5	100	76	1	[15]
ZSM-5	140	2	82.0	42.5	1	[33]
Acidic clays	50	2	99.9	15.7	1	[34]
Fe/MCM-41	70	2.5	57.5	26.8	1	[35]
HPW	140	3	100	90	1	[36]
Fe^{2+}-MCM	40	3	100	64	1	[37]
Formic Acid/Aniline	RT	1	100	76	1	[38]

[a]: selectivity for carveol, [b]: the numeral referring to total times in recycling use of typical catalyst.

There are few references regarding the investigation of catalyst stability in the catalytic rearrangement of α-epoxypinane and little detailed information on how these catalysts can be reused. Although some systems [13,15,36–38] have higher initial activity and carveol selectivity than the AC-COIMI-NH_4PW catalyst in this work, there are defects in the reusability of the catalyst. In the process of verifying the catalytic effect of HPW [36] in Table 3, it is found that there was severe gelatinization on the surface of HPW during the rearrangement reaction process. When entering the second round of reaction, the activity was decreased significantly and the conversion of α-epoxypinane was less than 30%. Based on the acid strength characteristics of other catalysts, it is inferred that these catalysts are difficult to reuse.

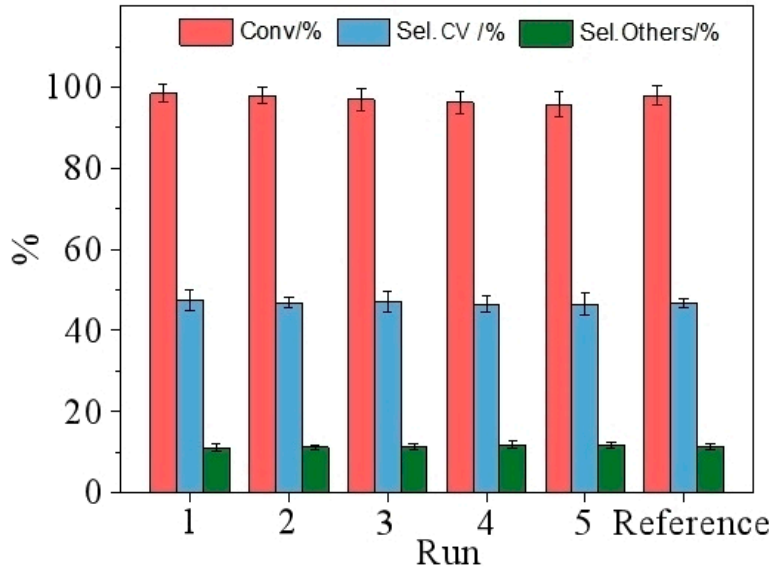

Figure 6. The reuse stability of AC-COIMI-NH_4PW.

The constructed ammonium ion of ammonium phosphotungstic acid supported on nitrogen-doped activated carbon on the AC-COIMI-NH_4PW catalyst has a dual structural feature in this work. Firstly, the organic amine base on the imidazole ring neutralizes one H^+ in the phosphotungstic acid molecule, and then the inorganic NH_3 base neutralizes the other two H^+ ions in the phosphotungstic acid molecule. When the constructed NH^{4+} acid center is used for the catalytic rearrangement of α-epoxypinane, due to the inhibition of the self-polymerization gelatinization side reaction of α-epoxypinane, the selectivity of carveol is improved and it exhibits a more distinctive catalytic performance than the relevant results elsewhere in the literature.

2.5. Plausible Mechanism of α-Epoxypinane Rearrangement

Based on the investigation of reaction conditions on the α-epoxypinane rearrangement, it was proposed that the mechanism involving the NH_4^+ acidic site cooperated with the solvent DMF on AC-COIMI-NH_4PW to catalyze the rearrangement is shown in Figure 7.

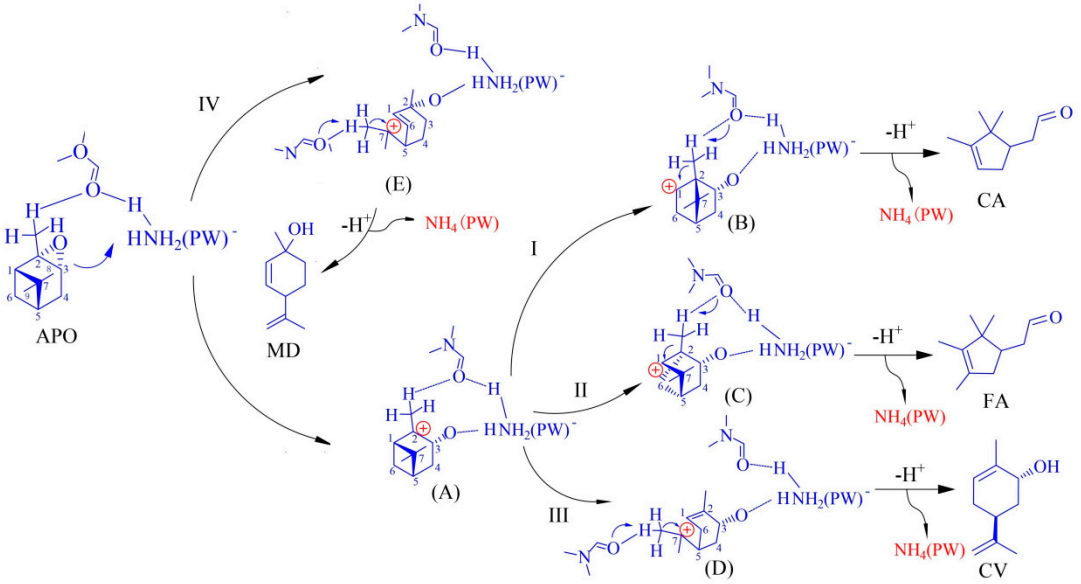

Figure 7. Route of α-epoxypinane rearrangement on AC-COIMI-NH_4PW (**A**–**E** are five kinds of intermediates).

Through the chemical adsorption of α-epoxypinane on the acidic sites over AC-COIMI-NH_4PW, the epoxy ring in α-epoxypinane is positively ionized on C2 through the acid-base interaction of the pair of nonbonding electrons in oxygen with the proton H^+ in NH_4^+, and a tertiary carbocation intermediate (A) is formed by breaking the ring. Subsequently, the carbocation intermediates undergo rearrangement assisted by the polarity and alkalinity of the solvent, which can be divided into three main reaction paths (I, II, and III) of the Wagner–Meerwein rearrangemen. Route I mainly occurs on the strong acid catalytic center, and electron migration occurs after the C1-C7 bond is broken, electrons on C1 are transferred to the original C2, and then a new secondary carbocation intermediate (B) is formed. Then, the C2-C3 bond is broken by a proton, an electron pair is transferred, and then, the proton elimination reaction occurs to produce CA.

Route II occurs mainly via electrons on C1 transferred to the original C2, and then a new secondary carbocation intermediate (C) is formed. Then, the isomer FA of CA is produced through C2-C3 bond breaking, an electron pair is transferred, and a proton is eliminated. The main product in the rearrangement is CV on AC-COIMI-NH_4PW: it is indicated that intermediate A is more inclined to rearrange along route III.

After the C1-C7 bond is broken, the electron pair on C7 is transferred to the original C2. At the same time, protons are rapidly removed, and double bonds are formed between C1-C2 with the assistance of DMF, forming a thermodynamically controlled stable intermediate (D). Subsequently, the transfer of protons of the external methyl group was promoted by the solvent, and CV was formed by desorption from the acidic site. From Figure 5, it can be observed that a small amount of C6 product MD was generated in parallel during the rearrangement process, which might be due to the region-selective opening of epoxy bonds catalyzed by NH_4^+ acid in AC-COIMI-NH_4PW. When α-epoxypinane interacts with NH_4^+ on the catalyst along with the formation of A, the O-C3 bond also can be broken along the interaction of the pair of nonbonding electrons in oxygen with the proton H^+ in NH_4^+. Meanwhile, the hydrogen negative ions H^- with an electron pair on C8 transfer to the positive carbon ions on C3, then an adsorbed carbon cation intermediate E is formed by

breaking the bond of C1 with C7 and the proton transfer from C6 to C8. Finally, MD can then be formed through the deprotonation on the methyl group C8 or C9 of E to form a double bond, which is desorbed under the complexation of DMF.

3. Materials and Methods

3.1. Reagent and Materials

Activated carbon, hydrogen peroxide, ammonium hydroxide, acetonitrile, chloroform, and N,N-dimethylformamide were purchased from China National Pharmaceutical Group Chemical Reagent Co., Ltd. (Shanghi, China). 2-methylimidazole was bought from Shanghai WK ChemReagent Co., Ltd. (Shanghi, China). and phosphotungstic acid was obtained from Aladdin Biochemical Technology Co., Ltd., (Shanghi, China). All the reagents used were of analytical grade. 99% α-pinene and 98% α-epoxypinane were provided by Hunan Yongzhou Lihao Technology Co., Ltd. (Yongzhou China), while 30% hydrogen peroxide solution was obtained from Baling Branch of SINOPEC (Yueyang, China). All chemicals were used without further purification.

3.2. Preparation and Characterization of AC-COIMI-NH_4PW Catalysts

The nitrogen-doped activated carbon-supported phosphotungstic acid catalyst (AC-COIMI-HPW) was prepared according to previous studies [24] (Scheme 2). Generally, the carboxylated activated carbon (AC-COOH) was obtained from the oxidation of activated carbon (AC) with 50% hydrogen peroxide and 12 mol/L^{-1} H_2SO_4 aqueous solution at 80 °C, then filtered, washed, and dried. The imidazolized activated carbon (AC-COIMI) was prepared through the direct imidazolization of AC-COOH with 2-methylimidazole at 180 °C, then washed with acetone and dried. The designed catalyst (AC-COIMI-HPW) from HPW bonded to the surface was made by the adsorption of HPW on the basic site of AC-COIMI in the aqueous solution, then washed with ultrapure water until no phosphotungstic acid existed in the aqueous phase, and dried in vacuo overnight.

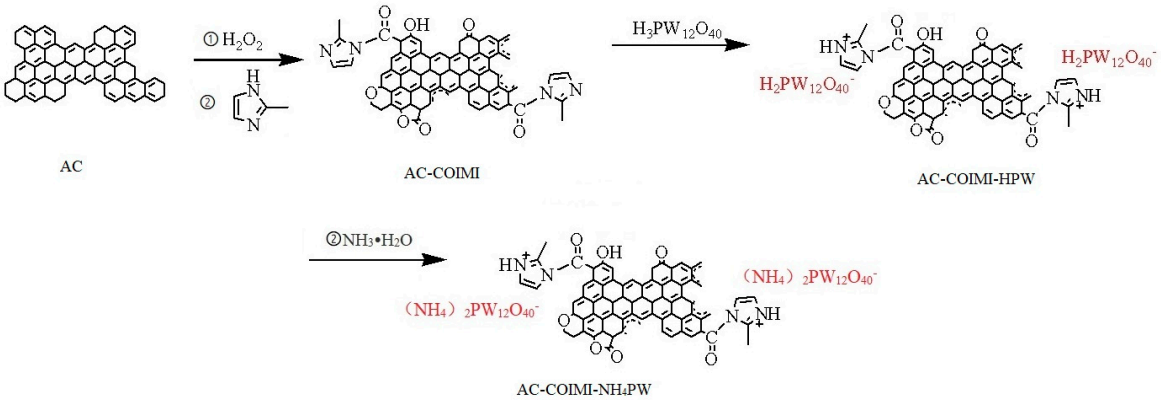

Scheme 2. Synthesis of the AC-COIMI-NH_4PW.

AC-COIMI-NH_4PW was prepared by weakening acidic sites of AC-COIMI-HPW using ammonification. Specific operation method: A beaker containing 20 mL of concentrated ammonia water was placed in a closed dryer. 2.0 g of the AC-COIMI-HPW catalyst was weighed and placed in a surface dish on the separator of the dryer. The catalyst was ammonia-smoked for 24 h at room temperature and dried overnight in a vacuum.

3.3. Rearrangement of α-Epoxypinane

A double-necked flask filled with 50 mg of AC-COIMI-NH_4PW, 10 mL of DMF, and 10 mmol of α-epoxypinane were mixed thoroughly and placed in an oil bath at 90 °C. After 2 h of reaction, crude carveol was obtained. Then the reaction flask was naturally cooled to room temperature and centrifuged at high speed to separate the catalyst particles. The supernatant liquid is sealed in the sample tube and placed in the freezer for analysis. The

qualitative analysis of rearrangement products, comparing with standard items was run by Shimadzu GC-MS-QP2010 (Shimadzu, Changsha, China), and the quantitative analysis using the internal standard method by Shimadzu GC-2010, HP-5 capillary (0.32 mm × 30 m), with temperature programmed operation 80 °C (2 min) →10 °C·min^{-1}→180 °C (5 min).

3.4. Characterization of AC-COIMI-NH$_4$PW

FTIR of catalyst samples was performed in a Nicolet 370 infrared spectrophotometer using the KBr pellet technique with a range of 400–4000 cm^{-1}. XRD patterns were recorded by the Bruker D8 Advance diffractometer (Bruker Corporation, Beijing, China) within a range of 5°–60° and a sweep speed of 10°/min. The TG data of the sample were obtained by a PerkinElmer STA 6000 (Rigaku Asia Pacific PTE Ltd. Beijing, China)simultaneous thermal analyzer under a nitrogen atmosphere within a temperature range of 30 °C~200 °C at 10 °C/min. SEM imaging of the sample was performed on a Zeiss Sigma 300scanning electron microscope (Carl Zeiss GMBH, Guangzhou, China)with magnification ranging between 50–10,000 times. The BET surface area of the sample was determined with the Micromeritics ASAP 2460 (Micromeritics, Shanghai, China)surface area analyzer by the adsorption of nitrogen at 77.3K, P/P_0 = 0.000~0.994. In order to evaluate the XPS data, the Thermo Scientific Avantage software (version 4.88, Waltham, MA, USA) was applied. Deconvolution of HR XPS spectra was performed by applying a smart-type background and a Gaussian peak shape with 35% Lorentzian character. The measured binding energies were corrected relative to the energy of carbon peak (C1s) at 284.6 eV.

3.5. Reusing of the Catalyst

The mixture at the end of each reaction is transferred to a centrifugal tube, centrifuged on a high-speed centrifuge for 10 min, and then poured out. The AC-COIMI-NH$_4$PW catalyst on the wall of the centrifugal tube is transferred to the reaction bottle with ultrasonic assistance and the new round of reaction is performed. After the reaction was repeated 5 times, the collected catalyst was washed with petroleum ether three times, vacuum dried at 60 °C for 24 h, and then the reaction was carried out for the sixth time with adding fresh catalyst to make up the initial mass.

4. Conclusions

Based on designing the active components of the catalyst and evaluating the effect of solvents on the catalytic rearrangement of α-epoxypinane, it is found that ammonium phosphotungstate bonded with animidazole basic site on nitrogen-doped activated carbon AC-COIMI-NH$_4$PW presented an excellent catalytic performance for the rearrangement of α-epoxypinane in DMF as a solvent, in which the selectivity of carveol was as high as 50.6%. During the reusing of the catalyst, there was no loss of catalytic active sites, but there was a slight loss of catalyst quality during the stirring reaction operation. The catalytic performance of the reused catalyst can be restored to its original state by restocking an equal amount of fresh catalyst. A parallel catalytic mechanism from four main reaction paths is more suitable for the main product from the rearrangement of α-epoxypinane on AC-COIMI-NH$_4$PW.

Author Contributions: Conceptualization, X.L. and D.Y.; methodology, X.L. and D.Y.; software, M.Z. and P.Z.; resources, X.L. and D.Y.; data curation, M.Z. and H.L.; writing—original draft preparation, M.Z., S.R.K., H.L. and P.Z.; writing—review and editing, M.Z., S.R.K. and Y.Y.; visualization, M.Z. and P.Z.; supervision, M.Z. and H.L.; project administration, M.Z. and X.L.; funding acquisition, D.Y. All authors have read and agreed to the published version of the manuscript.

Funding: This research was funded by the National Natural Science Foundation of China grant number (22278122) and Key scientific and technological R&D projects in Hunan Province grant number (2015NK3029).

Data Availability Statement: Data are contained within the article.

Conflicts of Interest: The authors declare no conflicts of interest.

References

1. Bhatia, S.P.; McGinty, D.; Letizia, C.S.; Api, A.M. Fragrance material review on carveol. *Food Chem. Toxicol.* **2008**, *46*, 85–87. [CrossRef] [PubMed]
2. Alattar, A.; Alvi, M.A.; Rashid, S.; Hussain, N.; Gul, M.; Ikram, M.; Khalil, A.A.K.; Alshaman, R.; Shah, F.A.; Li, S.; et al. Carveol ameliorates mercury-induced oxidative stress, neuroinflammation, and neurodegeneration in a mouse brain. *NeuroToxicology* **2022**, *92*, 212–226. [CrossRef] [PubMed]
3. Noma, Y.; Asakawa, Y. Enantio and diastereoselectivity in the biotransformation of carveols by Euglena gracilis. Z. *Phytochemistry* **1992**, *31*, 2009–2011. [CrossRef]
4. Ain, R.; Elmar, A.; Anne, O.; Tiiu, K.; Mati, M. Composition of the essential oil of Levisticum officinale WDJ Koch from some European countries. *J. Essent. Oil Res.* **2008**, *20*, 318–322. [CrossRef]
5. Ahmed, M.S.; Khan, A.U.; Kury, L.T.A.; Shah, F.A. Computational and pharmacological evaluation of carveol for antidiabetic potential. *Front. Pharmacol.* **2020**, *11*, 1677–1684. [CrossRef]
6. Zhu, S.; Xu, S.; Yi, X.; Wang, J.; Zhao, Z.; Jiang, J. High value-added application of turpentine as a potential renewable source for the synthesis of heterocyclic schiff base derivatives of cis-1,8-p-menthane-diamine serving as botanical herbicides. *Ind. Crops Prod.* **2018**, *115*, 111–116. [CrossRef]
7. Salvador, V.T.; Silva, E.S.; Gonçalves, P.G.C.; Cella, R. Biomass transformation: Hydration and isomerization reactions of turpentine oil using ion exchange resins as catalyst. *Sustain. Chem. Pharm.* **2020**, *15*, 100214. [CrossRef]
8. Ljunggren, J.; Bylund, D.; Jonsson, B.G.; Edman, M.; Hedenström, E. Antifungal efficiency of individual compounds and evaluation of non-linear effects by recombining fractionated turpentine. *Microchem. J.* **2020**, *153*, 104325. [CrossRef]
9. Merghni, A.; Lassoued, M.A.; Rasoanirina, B.N.V.; Moumni, S.; Mastouri, M. Characterization of Turpentine nanoemulsion and assessment of its antibiofilm potential against methicillin-resistant Staphylococcus aureus. *Microb. Pathog.* **2022**, *166*, 105530. [CrossRef]
10. Patil, M.V.; Yadav, M.K.; Jasra, R.V. Catalytic epoxidation of α-pinene with molecular oxygen using cobalt (II)-exchanged zeolite Y-based heterogeneous catalysts. *J. Mol. Catal. A Chem.* **2007**, *277*, 72–80. [CrossRef]
11. Raupp, Y.S.; Yildiz, C.; Kleist, W.; Meier, M.A.R. Aerobic oxidation of α-pinene catalyzed by homogeneous and MOF-based Mn catalysts. *Appl. Catal. A Gen.* **2017**, *546*, 1–6. [CrossRef]
12. Maharana, T.; Nath, N.; Pradhan, H.C.; Mantri, S.; Routaray, A.; Sutar, A.K. Polymer-supported first-row transition metal schiff base complexes: Efficient catalysts for epoxidation of alkenes. *React. Funct. Polym.* **2022**, *171*, 105142. [CrossRef]
13. Costa, V.V.; Rocha, K.A.S.; Sousa, L.F.; Dutenhefner, P.A.R.; Gusevskaya, E.V. Isomerization of α-pinene oxide over cerium and tin catalysts: Selective synthesis of carveol and trans-sobrerol. *J. Mol. Catal. A Chem.* **2011**, *345*, 69–74. [CrossRef]
14. Ribeiro, C.J.A.; Pereira, M.M.; Kozhevnikova, E.F.; Kozhevnikov, I.V.; Gusevskaya, E.V.; Rocha, K.A.S.R. Heteropoly acid catalysts in upgrading of biorenewables: Synthesis of para-menthenic fragrance compounds from α-pinene oxide. *Catal. Today* **2020**, *344*, 166–170. [CrossRef]
15. Singh, A.S.; Naikwadi, D.R.; Ravi, K.; Biradar, A.V. Chemoselective isomerization of α-pinene oxide to carveol by robust and mild Brønsted acidic zirconium phosphate catalyst. *Mol. Catal.* **2022**, *521*, 112189. [CrossRef]
16. Barakov, R.; Shcherban, N.; Mäki-Arvela, P.; Yaremov, P.; Bezverkhyy, I.; Wärnå, J.; Murzin, D.Y. Hierarchical Beta zeolites as catalysts in α-pinene oxide isomerization. *ACS Sustain. Chem. Eng.* **2022**, *10*, 6642–6656. [CrossRef]
17. Valvekens, P.; Bloch, E.D.; Long, J.R.; Ameloot, R.; Vos, D.E. Counteranion effects on the catalytic activity of copper salts immobilized on the 2,2′-bipyridine-functionalized metal-organic framework MOF-253. *Catal. Today* **2015**, *246*, 55–59. [CrossRef]
18. Sundaravel, B.; Babu, C.M.; Vinodh, R.; Cha, W.S.; Jang, H.T. Synthesis of campholenic aldehyde from α-pinene using bi-functional PrAlPO-5 molecular sieves. *J. Taiwan. Inst. Chem. Eng.* **2016**, *63*, 157–165. [CrossRef]
19. Sidorenko, A.Y.; Aho, A.; Ganbaatar, J.; Batsuren, D.; Utenkova, D.B.; Sen'kov, G.M.; Wärnå, J.; Murzin, D.Y.; Agabekov, V.E. Catalytic isomerization of α-pinene and 3-carene in the presence of modified layered aluminosilicates. *Mol. Catal.* **2017**, *443*, 193–202. [CrossRef]
20. Sánchez-Velandia, J.E.; Agudelo-Cifuentes, A.; Villa, A.L. Kinetics of the isomerization of α-pinene epoxide over Fe supported MCM-41 and SBA-15 materials. *React. Kinet. Mech. Catal.* **2019**, *128*, 1005–1028. [CrossRef]
21. Sánchez-Velandia, J.E.; Gelves, J.F.; Márquez, M.A.; Dorkis, L.; Villa, A.L. Catalytic isomerization of α-pinene epoxide over a natural zeolite. *Catal. Lett.* **2020**, *150*, 3132–3148. [CrossRef]
22. Singh, A.S.; Advani, J.H.; Biradar, A.V. Phosphonate functionalized carbon spheres as Brønsted acid catalysts for the valorization of bio-renewable α-pinene oxide to carveol. *Dalton Trans.* **2020**, *21*, 7210–7217. [CrossRef] [PubMed]
23. Vrbková, E.; Vyskocilová, E.; Lhotka, M.; Cervený, L. Solvent influence on selectivity in α-pinene oxide isomerization using MoO_3-Modified aeolite BETA. *Catalysts* **2020**, *10*, 1244. [CrossRef]
24. Zheng, M.; He, H.; Li, X.Z.; Yin, D.L. Imidazolized activated carbon anchoring phosphotungstic acid as recyclable catalyst for oxidation of alcohols with aqueous hydrogen peroxide. *Front. Chem.* **2022**, *10*, 925622. [CrossRef] [PubMed]
25. Zheng, M.; Li, X.Z.; Xun, Y.Y.; Wang, J.H.; Yin, D.L. Selective catalytic epoxidation–hydration of α-pinene with hydrogen peroxide to sobrerol by durable ammonium phosphotungstate immobilized on imidazolized activated carbon. *Nanomaterials* **2023**, *13*, 1554. [CrossRef] [PubMed]
26. Advani, J.H.; Singh, A.S.; Khan, N.U.; Bajaj, H.C.; Biradar, A.V. Black yet green: Sulfonic acid functionalized carbon as an efficient catalyst for highly selective isomerization of α-pinene oxide to carveol. *Appl. Catal. B Environ.* **2020**, *268*, 118456. [CrossRef]

27. Liu, W.Z.; Guo, R.K.; Peng, G.M.; Yin, D.L. Sulfuric acid immobilized on activated carbon aminated with ethylenediamine: An efficient reusable catalyst for the synthesis of acetals (ketals). *Nanomaterials* **2022**, *12*, 1462. [CrossRef]
28. He, H.T.; Zheng, M.; Liu, Q.; Liu, J.; Zhao, J.; Zhuang, Y.T.; Liu, X.X.; Xu, Q.; Steven, R.K.; Yin, D.L. Hydroxyl-assisted selective epoxidation of perillyl alcohol with hydrogen peroxide by vanadium-substituted phosphotungstic acid hinged on imidazolyl activated carbon. *New J. Chem.* **2022**, *46*, 6636–6645. [CrossRef]
29. Li, J.; Zhang, J.; Wang, Y.; Wang, H.; Song, H. Preparation of highly active g-C3N4 supported amphiphilic quaternary ammonium phosphotungstate catalyst for solvent-free oxidative desulfurization of benzothiophene. *React. Kinet. Mech. Catal.* **2022**, *135*, 219–231. [CrossRef]
30. Toledo, R.B.C.; Aragón-Tobar, C.F.; Gámez, S.; Torre, E. Reactivation process of activated carbons: Effect on the mechanical and adsorptive properties. *Molecules* **2020**, *25*, 1681. [CrossRef]
31. Li, H.; Liu, J.; Zhao, J.; He, H.; Jiang, D.; Kirk, S.R.; Xu, Q.; Liu, X.; Yin, D. Selectively catalytic isomerization of β-pinene oxide to perillyl alcohol enhanced by tetra-imidazole nitrate ionic liquid. *Chemistryopen* **2021**, *10*, 477–485. [CrossRef] [PubMed]
32. Maki-Arvela, P.; Shcherban, N.; Lozachmeur, C.; Russo, V.; Warna, J.; Murzin, D.Y. Isomerization of α-pinene oxide: Solvent effects, kinetics and thermodynamics. *Catal. Lett.* **2019**, *149*, 203–214. [CrossRef]
33. Shcherban, N.D.; Barakov, R.Y.; Mäki-Arvela, P.; Sergiienko, S.A.; Bezverkhyy, I.; Eränen, K.; Murzin, D.Y. Isomerization of α-pinene oxide over ZSM-5 based micro-mesoporous materials. *Appl. Catal. A Gen.* **2018**, *560*, 236–247. [CrossRef]
34. Sidorenko, A.Y.; Kravtsova, A.V.; Aho, A.; Heinmaa, I.; Kuznetsova, T.F.; Murzin, D.Y.; Agabekov, V.E. Catalytic isomerization of α-pinene oxide in the presence of acid-modified. *Mol. Catal.* **2018**, *448*, 18–29. [CrossRef]
35. Sanchez-Velamdia, J.E.; Villa, A.L. Selective synthesis of high-added value chemicals from α-pinene epoxide and limonene epoxide isomerization over mesostruc- tured catalysts: Effect of the metal loading and solvent. *Catal. Today* **2021**, *394–396*, 208–218. [CrossRef]
36. Rocha, K.S.; Hoehne, J.L.; Gusevskaya, E.V. Phosphotungstic acid as a versatile catalyst for the synthesis of fragrance compounds by α-pinene oxide isomerization: Solvent-induced chemoselectivity. *Chem.-A Eur. J.* **2008**, *14*, 6166–6172. [CrossRef]
37. Coelho, J.V.; Meireles, A.L.P.M.; Rocha, K.A.S.; Pereira, M.C.; Oliveira, L.C.A.; Gusevskaya, E.V. Isomerization of α-pinene oxide catalyzed by iron-modified mesoporous silicates. *Appl. Catal. A Gen.* **2012**, *443–444*, 125–132. [CrossRef]
38. Ravi, K.; Naikwadi, D.R.; Bankar, B.D.; Biradar, A.V. Sustainable isomerization of α-pinene oxide to trans-carveol using formic acid/aniline system at room temperature. *Adv. Sustain. Syst.* **2021**, *5*, 00212. [CrossRef]